Supplemental Figure legends

Figure S1 Assessment of linear quantitation range for emPAI spectral counting and selected reaction monitoring (SRM). Bovine serum albumin (BSA) tryptic digest was spiked into the *P. aeruginosa* tryptic digest at a ratio from 1:10 – 1:10,000 (w/w) as shown. A) emPAI spectral counting demonstrated over three orders of magnitude linear range to quantify BSA peptides. It is noted that at the 1:10,000 dilution point fewer than three minimal unique peptides from BSA were quantified. PA1800 trigger factor (Tig) showed constant levels of *P. aeruginosa* proteins in different BSA dilution points. B) SRM demonstrates four orders of magnitude linear quantitation range for three BSA peptides.

Figure S2 Assessment of coefficient of variation (CVs) of spectral counting measurement by emPAI. Exponentially Modified Protein Abundance Index (emPAI) was used as spectral counting method (1). The CV of each protein emPAI was calculated from seven replicate analyses in dosage treatment or 5 replicate analyses of the time course treatment. Approximate 40% median CV was found. The tight CV is useful to distinguish small protein fold change (Figure S5).

Figure S3 Protein quantitation correlation of spectral counting and SRM. The fold change for ten proteins (IbpA, ClpB, DnaK, PA0779, HslU, HslV, DhcB, BkdB, TufA, Tig) at different tobramycin treatment conditions were compared. X axis: protein fold change quantified by spectral counting. Y axis: protein fold change by SRM, which was the average of the peptide ratio. A) The full range (0 to 100 fold change) and all quantitation points are shown. A close to 45° linear regression relationship with the correlation coefficient of R^2=0.96 was observed, indicating the strong quantitation correlation. B) To further validate the correlation, four IbpA quantitation points (highest fold changes) were removed, and the linear correlation was reassessed. The remaining quantitation points also indicate a linear correlation of R^2=0.61.

Figure S4 Comparison of tobramycin responsive genes in transcriptomics (2) and proteomics analyses. A total of eleven common tobramycin induced genes at both mRNA and protein levels were identified, they were: *IbpA*, *ClpB*, *PA0779*, *HslU*, *HslV*, *PA4971*, *GshA*, *PA4061*, *GrpE*, *DnaJ* and *PA4842*. Other tobramycin responsive genes detected at the RNA level were not able to be quantified by proteomics, probably due to the low abundance of protein. The y axis for transcriptomics data was the hybridization intensity ratio of +/- Tob, and for proteomics data was the emPAI ratio of Tob_{15min}/CK and Tob_{60min}/CK. The x axis was the protein rank number by high to low fold change of RNA. RNA data was compared to proteomics data from 15 min and 60 min treatments. At the time point of 15 min, a general higher fold change was observed at the RNA level. However, at the time point of 60 min, the fold change of many proteins exceeded their RNA fold change level, suggesting post-transcriptional regulation for these proteins in tobramycin treatment. The overall direction of change for the tobramycin up-regulated genes appeared to be consistent between RNA and proteins, but no strong correlation was observed in terms of the extent of the fold change (R^2=0.34).

Figure S5 Validation of statistically altered proteins of small fold change. It is noted that a number of proteins lower than 2 fold spectral counting changes were detected as statistically altered proteins. We used three different approaches to verify whether these statistical changes are real. A) We found that most of these proteins were quantified by more than five unique peptides. Higher spectral counts can be translated as higher statistical power, thus enabled the differentiation of small fold changes. Plotting the emPAI values with 95% confidence intervals recapitulates these statistical differences. B) We developed SRM assays to examine the small fold changes for some of these proteins. In the case of GroEL and Lon, their small but significant changes were unequivocally confirmed. C) We manually extracted the ion chromatogram (XIC) for precursor ions of peptides for some of these proteins. In the examples of GroEL, FaoA and MexE, the

results of XIC also showed consistent changes with spectral counting results. In addition, we examined the biological functions of these low but statistically significant level fold change proteins, and found in many cases the biological functions of these proteins were related to the functions of many high fold change proteins. Thus, this group of small but statistically significantly changed proteins was substantiated and was included in the functional analysis. Statistical significance of the fold change is indicated with red asterisk. TufA is shown as control and did not exhibit significant changes.

Figure S6 Gene ontology analysis for tobramycin down-regulated proteins. A) Overrepresented pathways for proteins down-regulated in the tobramycin dosage experiments. The statistic test was analyzed in BiNGO as described in Figure 4. The y-axis significance value was converted from P value by taking log10, and the corresponding 0.01 and 0.05 significance levels are indicated in the figure. The pathways of carbon metabolism, nucleotide metabolism and proteins synthesis were statistically down-regulated in response to tobramycin. B) Overrepresented pathways for proteins that were down-regulated in the tobramycin time course treatment were consistent with the down-regulated pathways in dosage treatment.

Figure S7 Quantitative proteome network of proteins that were statistically decreased at 1.0 µg/ml tobramycin 360 min treatment. The protein fold change quantified by emPAI spectral counting is illustrated in green. Many proteins in the pathways of protein synthesis, nucleotide metabolism, glucose and TCA carbon metabolism and energy derivation and electron transport activities were statistically down-regulated at 1.0 µg/ml tobramycin after 360 min treatment.

Figure S8 Tobramycin minimal inhibitory concentration (MIC) assays for *P. aeruginosa* mutants. Tobramycin MIC assays were performed in two-fold dilution series in the range of 0.03 to 1.0 μg/ml. Sample loading map is illustrated in the 0.125 μg/ml series, and was kept the same for all concentrations. MPAO1 is the wild type control strain, PA3303 is the control strain for transposon insert. Strains shown in red are the transposon mutants for single-gene knockouts. PA0779 (a, b), *clpB* (a) and *hslV* (a, b, c) strains refer to PA0779 (PW2411, PW2414), *clpB* (PW86512), *hslV* (PW9487, PW9485, PW9486) (3). Single gene mutants also include Δ*ftsh* in-frame deletion mutant and *ibpa* inactivation mutant with *lux* insertion. *PKH181* is the control strain for lux insert. Double mutants were shown in blue, and three independent transformants (1,2,3 suffix) of each double mutant were assayed. Strains *ibpa*, *PKH181, PA3303* were spotted twice or three times per plate to examine the consistency in sample loading (approximately 10^5 cells were intended to load at per spot). MIC is the lowest concentration where the lawn growth of the spotted cell was abolished after 18 hours incubation at 37°C. In plates 0.03 μg/ml and 0.06 μg/ml, Δ*ftsh* mutant is highlighted, because it shows that inactivation of single *ftsH* gene causes *P. aeruginosa* to be hypersensitive to tobramycin as reported in Hinz et al. (4). In plate 0.25 μg/ml, *hslV* single mutant *ibpA/hslV* double mutants are highlighted, because *ibpA/hslV* double mutants show greater sensitivity to tobramycin compared to *ibpa* single mutant and *hslV* (PW9485, PW9486) mutants. In plate 0.5 μg/ml, *clpB and PA0779* single mutants, and *ibpA/clpB* and *ibpA/PA0779* double mutants are highlighted, because it shows that *ibpA/clpB* and *ibpA/PA0779* have higher sensitivity compared to single mutants *ibpa, clpB and PA0779*. Results were repeated with three transformants for each double mutant strain, and similar trend was observed (see Figure 7 for summarized results). It should be noted that we recently identified the genotype segregation of *mexT* allele that occurs in MPAO1 cells, which causes progenitor cells to have sensitivity changes in chloramphenicol resistance. While we confirmed that double mutant share the same *mexT r*-allele as *ibpa* mutants and MPAO1 strains, transposon single mutants *clpB, hslV* and *PA0779* contain *mexT s*-allele, and thus the tobramycin sensitivity changes of double mutants compared to *clpB, hslV* and *PA0779* should be taken with caution.

Supplemental References:

1. Ishihama Y, Oda Y, Tabata T, Sato T, Nagasu T, Rappsilber J, Mann M. Exponentially modified protein abundance index (emPAI) for estimation of absolute protein amount in proteomics by the number of sequenced peptides per protein. Mol Cell Proteomics. 2005;4(9):1265-72. doi: DOI 10.1074/mcp.M500061-MCP200. PubMed PMID: ISI:000231836100006.

2. Lee S, Hinz A, Bauerle E, Angermeyer A, Juhaszova K, Kaneko Y, Singh PK, Manoil C. Targeting a bacterial stress response to enhance antibiotic action. Proceedings of the National Academy of Sciences of the United States of America. 2009;106(34):14570-5. Epub 2009/08/27. doi: 10.1073/pnas.0903619106. PubMed PMID: 19706543 PMCID: PMC2732827.

3. Held K, Ramage E, Jacobs M, Gallagher L, Manoil C. Sequence-Verified Two-Allele Transposon Mutant Library for Pseudomonas aeruginosa PAO1. J Bacteriol. 2012;194(23):6387-9. doi: Doi 10.1128/Jb.01479-12. PubMed PMID: ISI:000310924300004.

4. Hinz A, Lee S, Jacoby K, Manoil C. Membrane Proteases and Aminoglycoside Antibiotic Resistance. J Bacteriol. 2011;193(18):4790-7. doi: Doi 10.1128/Jb.05133-11. PubMed PMID: ISI:000294261700024.

Figure S1

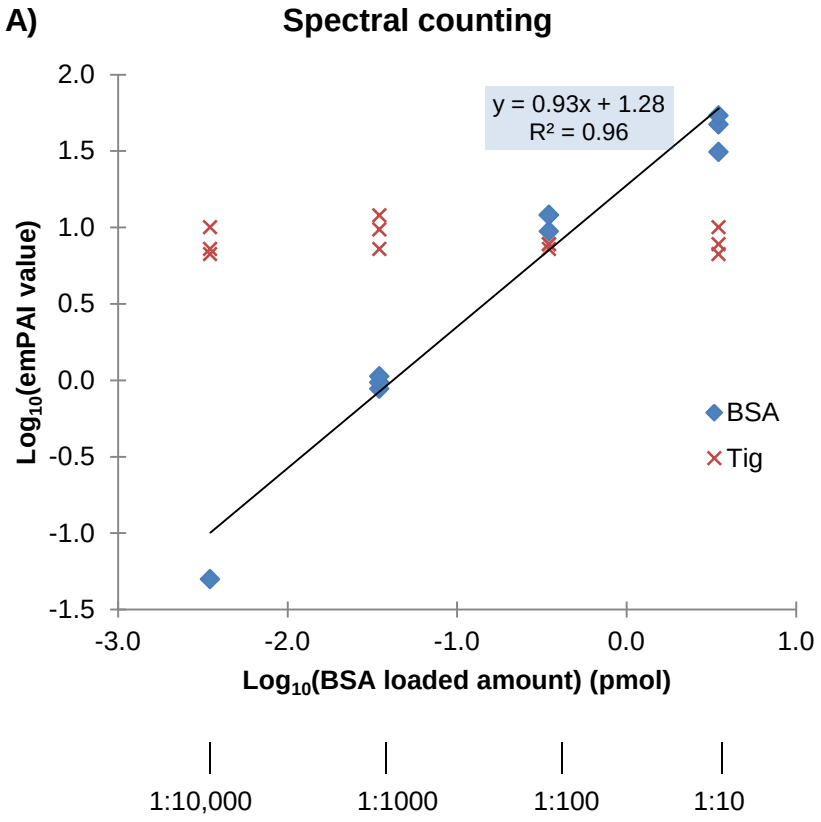
A)
Spectral counting
y = 0.93x + 1.28
R² = 0.96
BSA
Tig
Log10(empAI value)
Log10(BSA loaded amount) (pmol)
1:10,000
1:1000
1:100
1:10
BSA spiked in ratio
[BSA: PAO1 total proteins (µg:µg)]

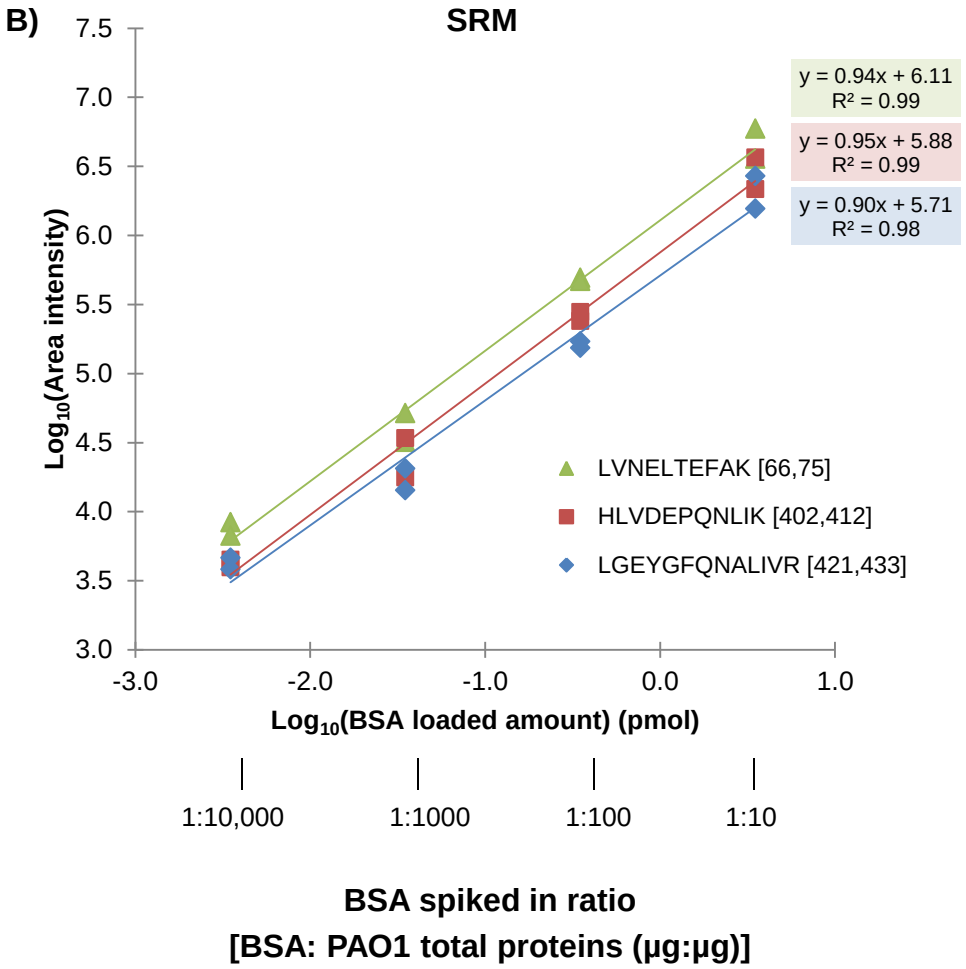
B)
SRM
y = 0.94x + 6.11
R² = 0.99
y = 0.95x + 5.88
R² = 0.99
y = 0.90x + 5.71
R² = 0.98
LVNELTEFAK [66,75]
HLVDEPQNLIK [402,412]
LGEYGFQNALIVR [421,433]
Log10(Area intensity)
Log10(BSA loaded amount) (pmol)
1:10,000
1:1000
1:100
1:10
BSA spiked in ratio
[BSA: PAO1 total proteins (µg:µg)]

Figure S2

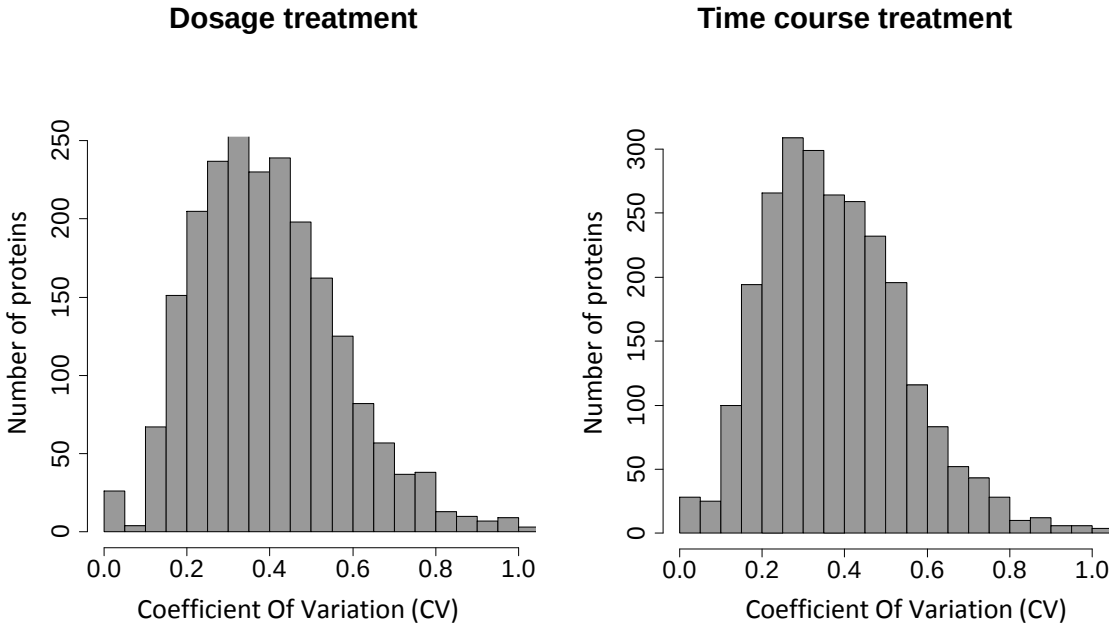
Dosage treatment
Number of proteins
0
50
100
150
200
250
0.0
0.2
0.4
0.6
0.8
1.0
Coefficient Of Variation (CV)

Time course treatment
Number of proteins
0
50
100
150
200
250
300
0.0
0.2
0.4
0.6
0.8
1.0
Coefficient Of Variation (CV)

Figure S3

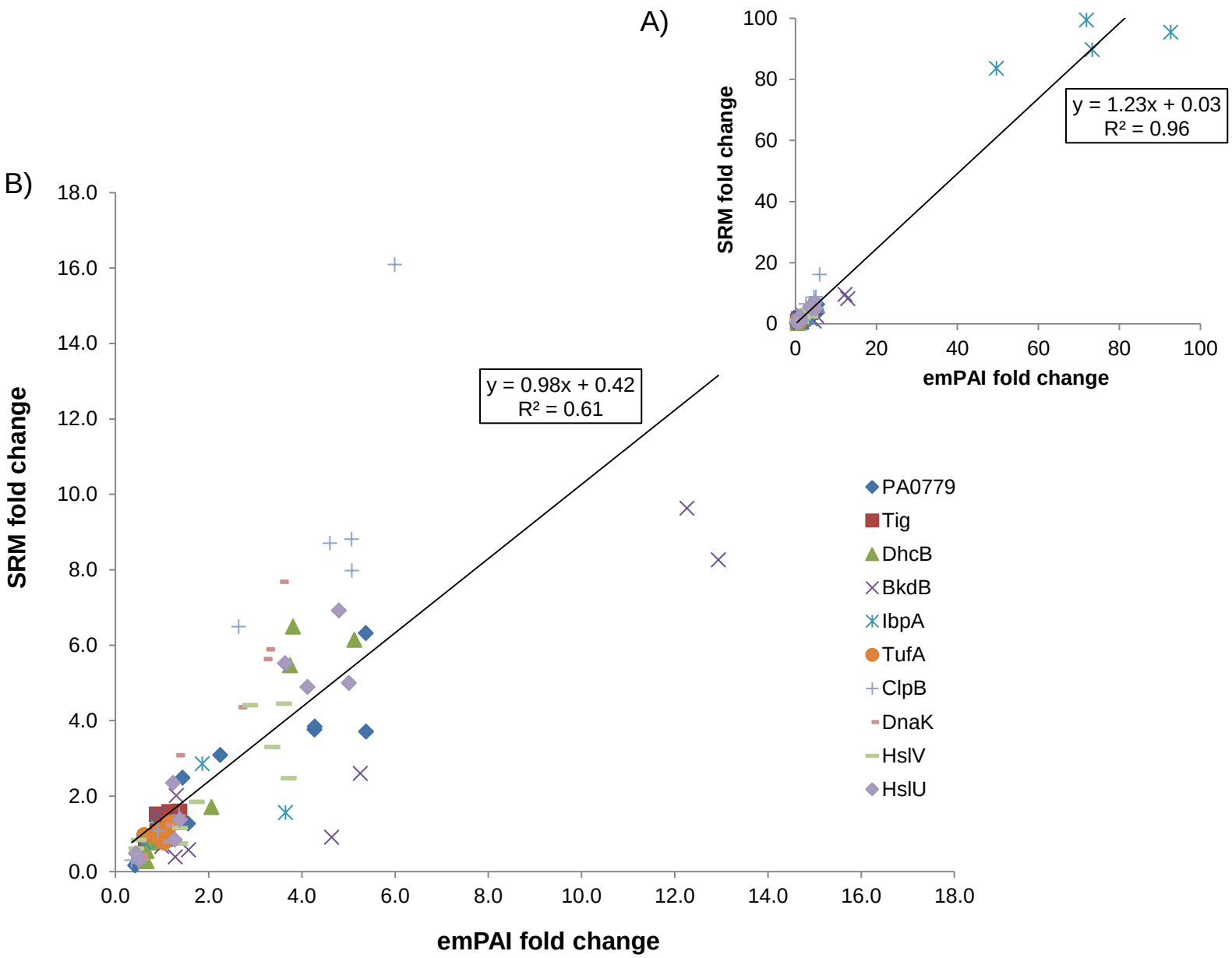
A)
SRM fold change
emPAI fold change
y = 1.23x + 0.03
R² = 0.96
B)
SRM fold change
emPAI fold change
y = 0.98x + 0.42
R² = 0.61
PA0779
Tig
DhcB
BkdB
IbpA
TufA
ClpB
DnaK
HslV
HslU

Figure S4

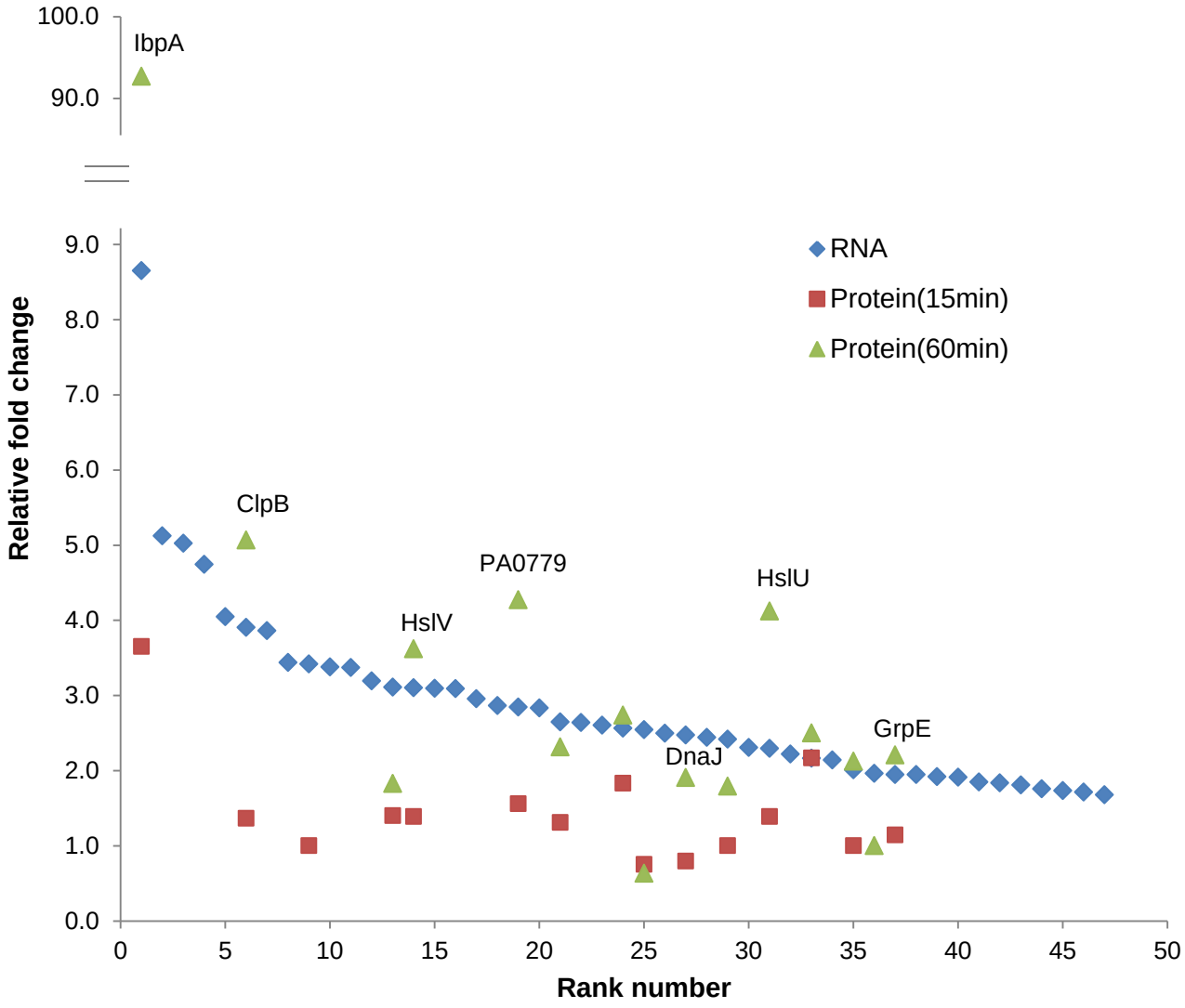
100.0
90.0
IbpA
9.0
8.0
7.0
6.0
5.0
4.0
3.0
2.0
1.0
0.0
Relative fold change
RNA
Protein(15min)
Protein(60min)
ClpB
PA0779
HslV
HslU
GrpE
DnaJ
0
5
10
15
20
25
30
35
40
45
50
Rank number

Figure S5

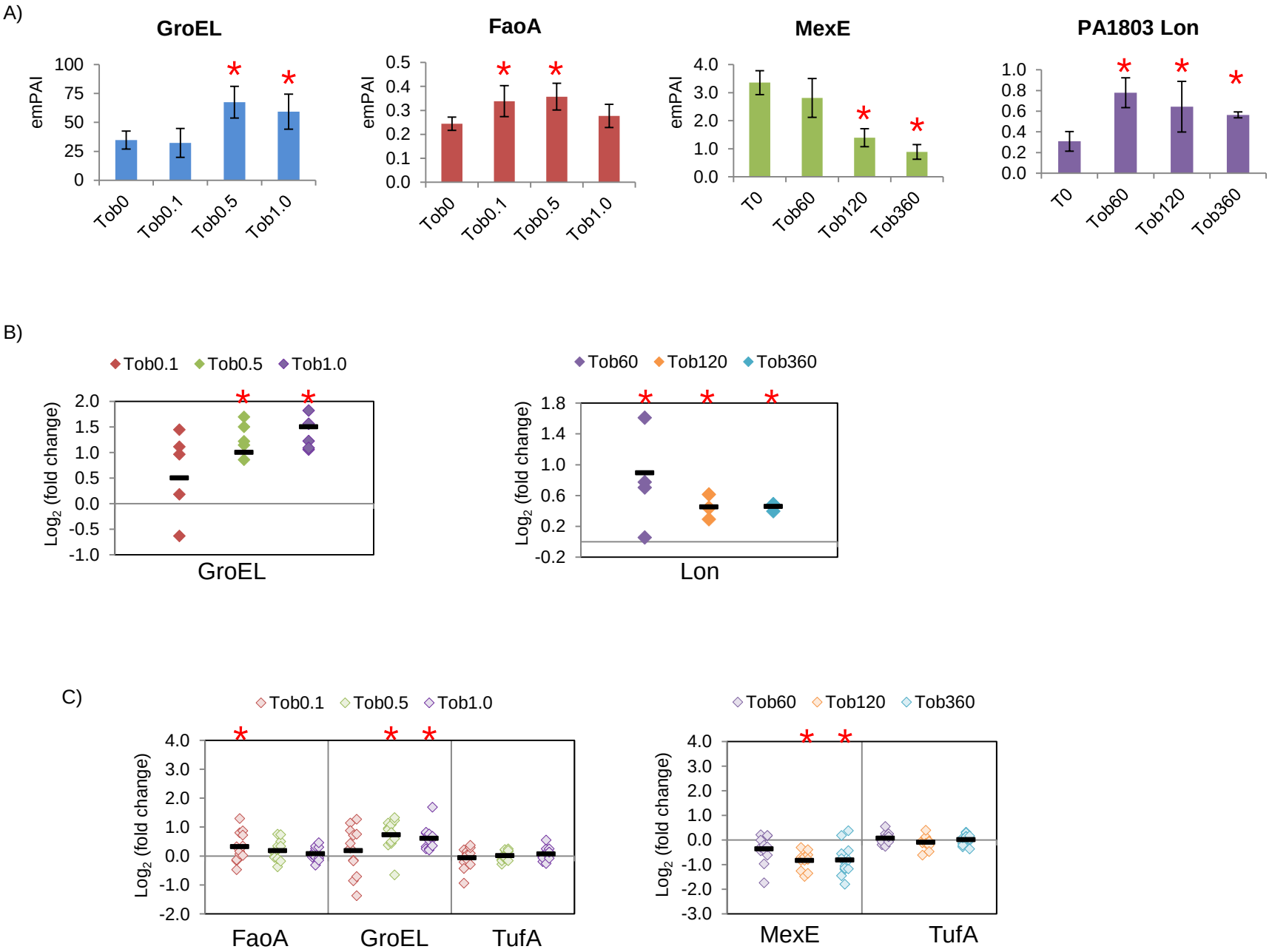
A)
GroEL
FaoA
MexE
PA1803 Lon
emPAI
Tob0
Tob0.1
Tob0.5
Tob1.0
T0
Tob60
Tob120
Tob360
B)
Log2 (fold change)
GroEL
Lon
C)
FaoA
GroEL
TufA
MexE
TufA

Figure S6

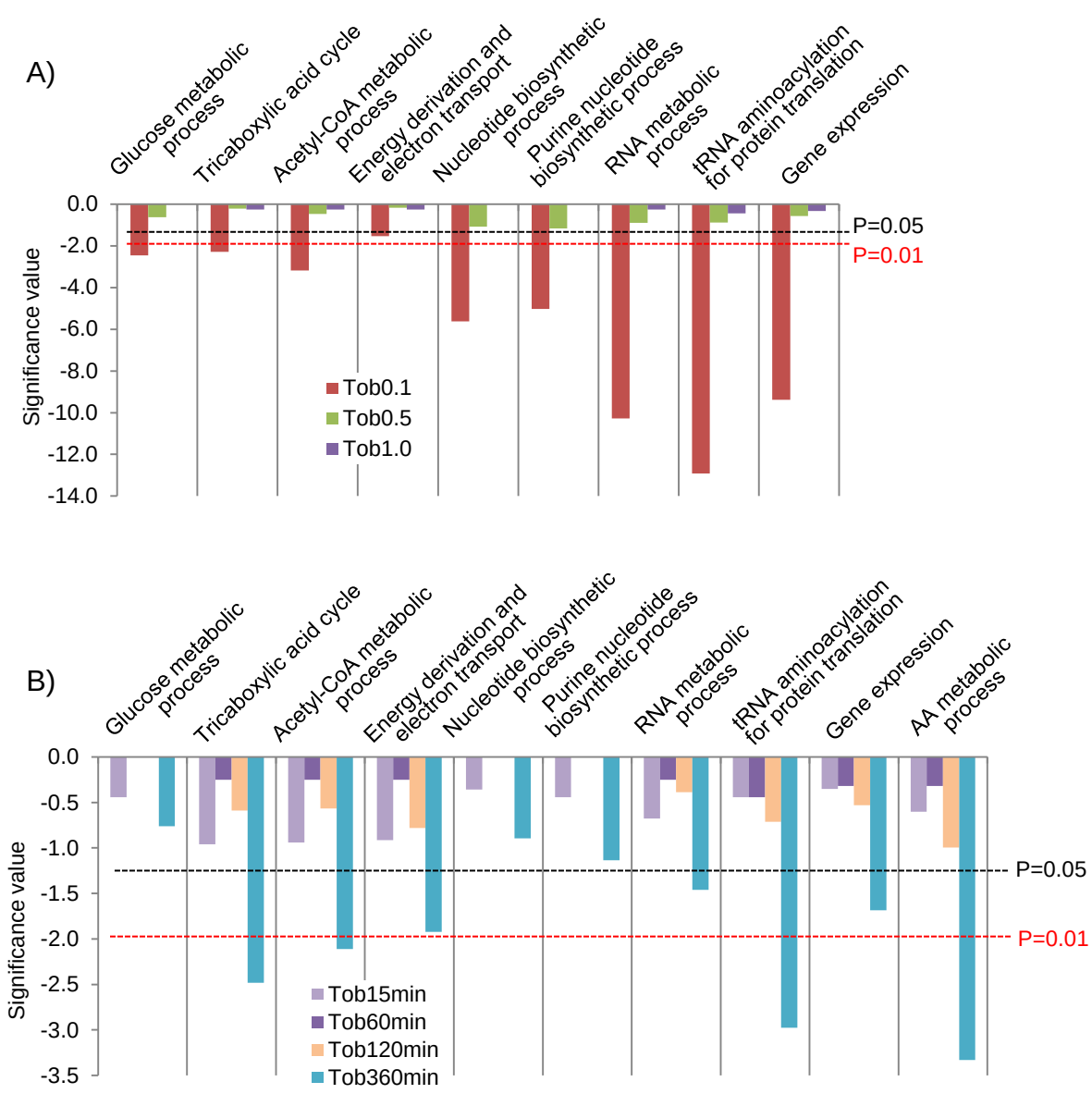
A)
Glucose metabolic process
Tricaboxylic acid cycle
Acetyl-CoA metabolic process
Energy derivation and electron transport
Nucleotide biosynthetic process
Purine nucleotide biosynthetic process
RNA metabolic process
tRNA aminoacylation for protein translation
Gene expression
Significance value
0.0
-2.0
-4.0
-6.0
-8.0
-10.0
-12.0
-14.0
P=0.05
P=0.01
Tob0.1
Tob0.5
Tob1.0
B)
Glucose metabolic process
Tricaboxylic acid cycle
Acetyl-CoA metabolic process
Energy derivation and electron transport
Nucleotide biosynthetic process
Purine nucleotide biosynthetic process
RNA metabolic process
tRNA aminoacylation for protein translation
Gene expression
AA metabolic process
Significance value
0.0
-0.5
-1.0
-1.5
-2.0
-2.5
-3.0
-3.5
P=0.05
P=0.01
Tob15min
Tob60min
Tob120min
Tob360min

Figure S7

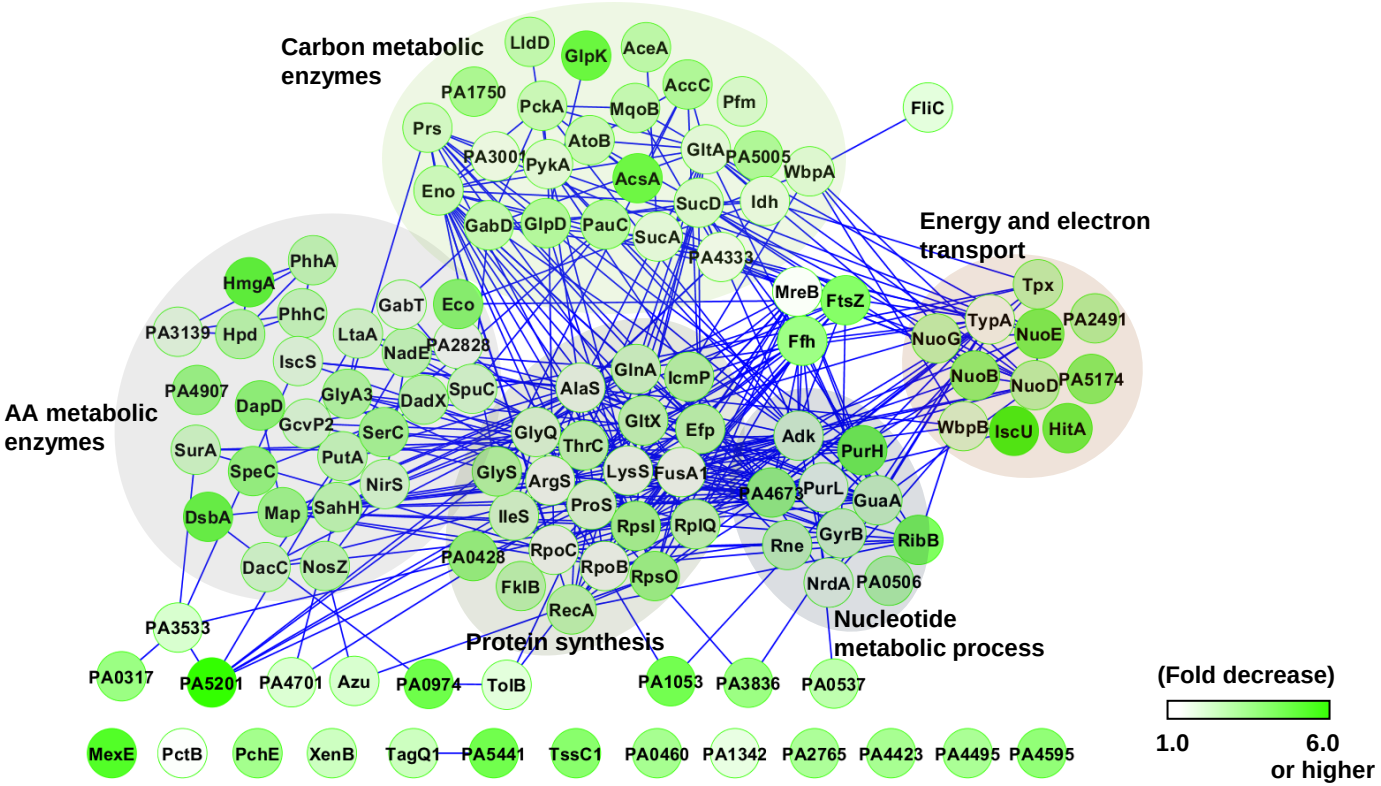
Carbon metabolic enzymes
Energy and electron transport
AA metabolic enzymes
Protein synthesis
Nucleotide metabolic process
LldD
GlpK
AceA
AccC
Pfm
FliC
PA1750
PckA
MqoB
Prs
AtoB
GltA
PA5005
WbpA
PA3001
PykA
AcsA
Eno
SucD
Idh
GabD
GlpD
PauC
SucA
PA4333
PhhA
HmgA
PhhC
GabT
Eco
MreB
FtsZ
Tpx
TypA
PA2491
NuoE
PA3139
Hpd
LtaA
NadE
PA2828
Ffh
NuoG
IscS
GlnA
IcmP
NuoB
NuoD
PA5174
PA4907
DapD
GlyA3
DadX
SpuC
AlaS
GcvP2
SerC
GlyQ
GltX
Efp
Adk
WbpB
IscU
HitA
SurA
ThrC
PurH
SpeC
PutA
GlyS
ArgS
LysS
FusA1
NirS
PA4678
PurL
GuaA
DsbA
Map
SahH
IleS
ProS
RpsI
RplQ
Rne
GyrB
RibB
DacC
NosZ
PA0428
RpoC
RpoB
RpsO
NrdA
PA0506
FklB
RecA
PA3533
PA0317
PA5201
PA4701
Azu
PA0974
TolB
PA1053
PA3836
PA0537
MexE
PctB
PchE
XenB
TagQ1
PA5441
TssC1
PA0460
PA1342
PA2765
PA4423
PA4495
PA4595
(Fold decrease)
1.0
6.0
or higher

Figure S8

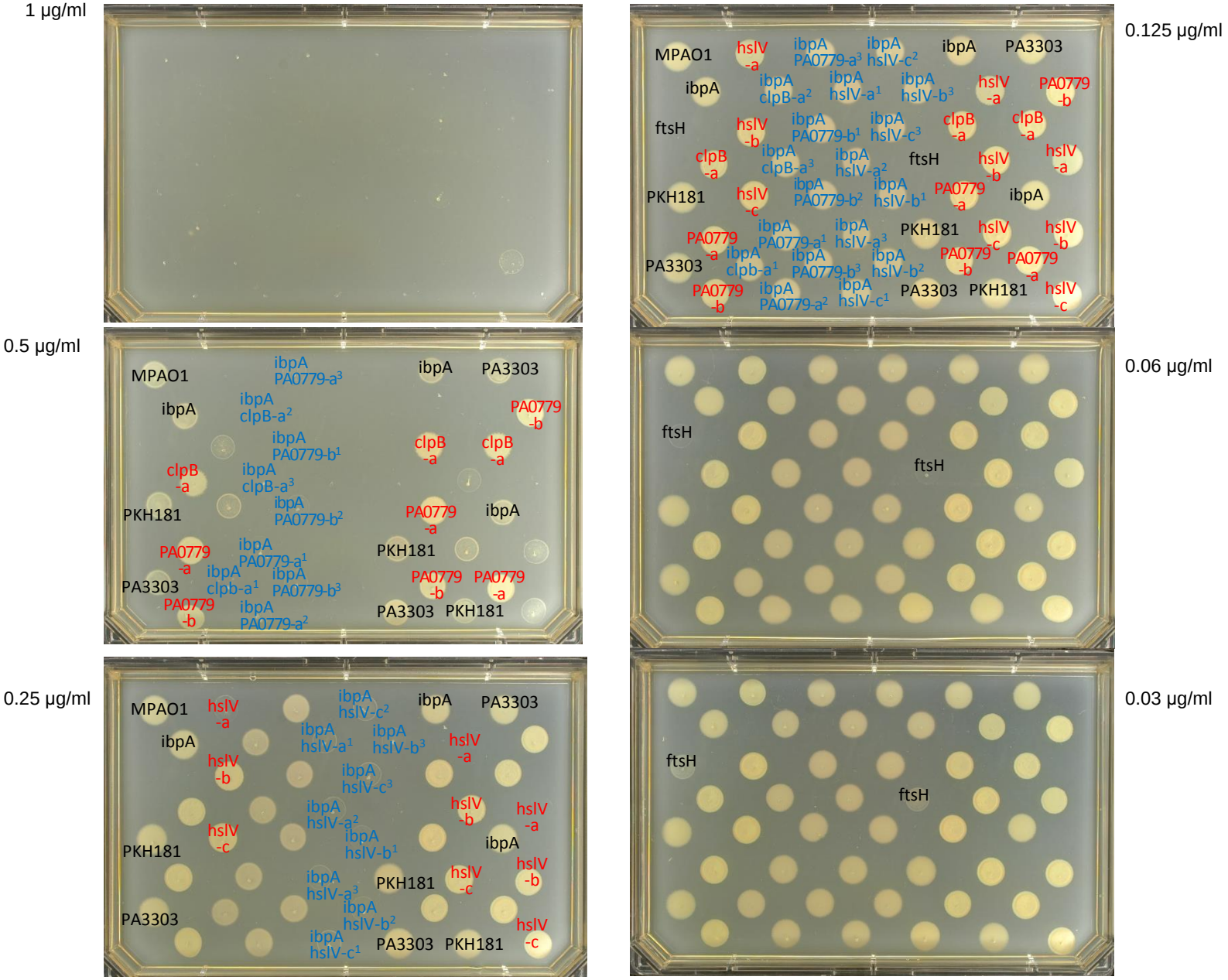
1 µg/ml
0.5 µg/ml
0.25 µg/ml
0.125 µg/ml
0.06 µg/ml
0.03 µg/ml
MPAO1
ibpA
PA3303
ftsH
PKH181
hslV -a
hslV -b
hslV -c
clpB -a
PA0779 -a
PA0779 -b
ibpA PA0779-a3
ibpA hslV-c2
ibpA clpB-a2
ibpA hslV-a1
ibpA hslV-b3
ibpA PA0779-b1
ibpA hslV-c3
ibpA clpB-a3
ibpA hslV-a2
ibpA PA0779-b2
ibpA hslV-b1
ibpA PA0779-a1
ibpA hslV-a3
ibpA clpb-a1
ibpA PA0779-b3
ibpA hslV-b2
ibpA PA0779-a2
ibpA hslV-c1